JOURNAL OF MATERIALS SCIENCE **38** (2003) 3567–3577

Co-continuous Al/Al_2O_3 composite produced by liquid displacement reaction: Relationship between microstructure and mechanical behavior

G. M. LA VECCHIA
Università di Brescia, Dipartimento di Ingegneria Meccanica, Brescia, Italy
E-mail: marina.lavecchia@unibs.it

C. BADINI, D. PUPPO
Politecnico di Torino, Dipartimento di Scienza dei Materiali e Ingegneria Chimica, Torino, Italy
E-mail: badini@athena.polito.it

F. D'ERRICO
Politecnico di Milano, Dipartimento di Meccanica, Milano, Italy
E-mail: fabrizio.derrico@polimi.it

Co-continuous 63%Al_2O_3/37%Al(Si) composite, known as C^4 composite, was produced by submersion of silica glass specimens in a molten metal bath. The effect of temperature and composition of the metal bath on the reactive penetration rate was investigated. An infiltration speed exceeding 2 mm/h, increasing with temperature, and suitable for practical applications, was observed above 1100°C. Mechanical properties of C^4 specimens were measured, at room temperature, and related to composite microstructure. This latter was investigated by optical and scanning electron microscopy, electron probe microanalysis, X-ray diffraction and porosimetry.

The strong interfacial bonds between metal and ceramic resulted in low thermal expansion, high stiffness, and good compression and bending strength. On the contrary, the composite showed a rather poor tensile strength, due to a high ceramic percentage and, partially, to porosity. In spite of the low ductility shown by the investigated composite, the metal network provides a toughening effect, which resulted in a ductile micro-mechanism of fracture, localized in the zones characterized by the presence of the metal matrix.

1. Introduction

Discontinuously reinforced metal matrix composites have been extensively studied for the past twenty years. The primary support for these composites has come from the aerospace industry for airframe and spacecraft components. More recently, automotive, electronic, and recreation industries have been working diffusely with these composites [1–3]. Developing of most of the existing composites has been going on the basis of their capability to be designed to provide the required material behavior. Aiming to decrease weight and to produce structural parts more resistant to thermal gradients than traditional aluminum alloys, many efforts are currently directed towards metal matrix composites (with low density aluminum, magnesium and titanium based matrices), even in presence with high percentages of ceramic reinforcement (>50%) [4–7]. Particularly, considering the automotive industry, where the maximum reinforcement percentage is about 30%, it is shown that the running costs are lower because of weight saving allowed by designing a part made of a composite material instead of traditional metal alloys [8]. For applications demanding high toughness, a proper choice of metal matrix, both in terms of chemical composition and percentage must be considered. Even the homogeneity of reinforcing particle distribution within the matrix must be evaluated in order to improve the mechanical properties. In particular, a higher fracture toughness can be obtained owing to a continuous and regular ceramic network throughout the microstructure. Contrary, distributing the same values of ceramic phase in the form of discrete particles embedded in a metallic matrix rather frequently promote the formation of reinforcement clusters, weak zones usually working as fracture initiation sites [9–11].

A new family of composites, called interpenetrating phase composites, or co-continuous ceramic composites (C^4), was developed by Breslin *et al*. These materials were produced by immersing a silica preform into molten aluminum without the application of external pressure [12]. The near-net shape capability of C^4 materials [13], along with low production costs, are further

advantages of co-continuous composites. During reactive metal infiltration, molten aluminum reduces the silica preform to produce a composite characterized by interpenetrated Al_2O_3 and metal matrix (Al or Al-Si alloy). The final material consists of approximately 70% interconnected alumina, which provides high stiffness, good strength and improved wear resistance with respect to aluminum matrix composites characterized by a lower percentage of reinforcement. The remaining 30% aluminum acts as a toughening phase and improves thermal and electrical conductivity.

This combination of properties, along with a good tribological performance [14–16], makes these materials very promising for applications such as automotive disk brake rotors and callipers, internal combustion engine piston crowns, cylinder liners, connecting rods, turbine compressors, robot arms, etc.

In this work an Al_2O_3/Al composite (containing about 67 vol% alumina), was fabricated by immersing silica preforms into molten Al, and then characterized in terms of microstructure and mechanical behavior (modulus of rupture, compression and tensile strength, fracture toughness, and hardness).

2. Experimental procedure

2.1. Materials and reactive metal penetration process

A Reactive Metal Penetration (RMP) method was adopted, using pure aluminum (99.9% wt) and an Al-10% Si alloy as infiltrating alloys. The latter one was prepared on a laboratory scale by melting together aluminum and high purity (99.9%) silicon, in order to avoid the presence of any other alloying elements, which could affect the penetration process.

Differently shaped specimens of silica glass were submitted to reactive infiltration, in air, with molten metal, in order to investigate the infiltration rate or to obtain composite samples for mechanical tests. For this reason both round bars (7.65 mm in diameter) and plates of $5 \times 10 \times 50$ mm^3 amorphous silica were used for composite fabrication. Highly purified, hydroxyl-ion-free quality, clear fused quartz, suitable for optical and electronic purposes, with less than 2.5 bubbles or inclusions per cubic decimeter, was used.

The investigation of the infiltration rate was carried out by using the apparatus shown in Fig. 1, which allows for the reactive metal penetration in the longitudinal direction of the silica glass bar. Checking the growth of the reaction layer at different times and temperatures

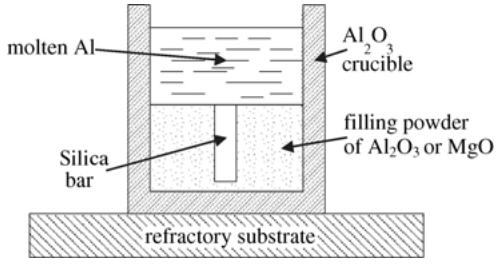

Figure 1 Experimental apparatus used for infiltration rate measurements (molten metal infiltrates silica glass bar parallel to longitudinal axis).

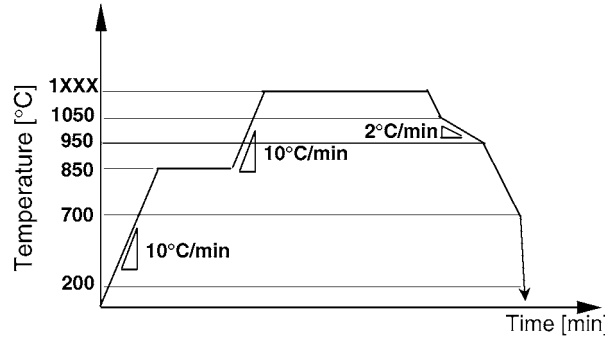

Figure 2 Thermal cycle used to study the infiltration rate and to obtain composite mechanical samples (1xxx°C equal to 1100°C or 1200°C, according to the test holding temperature).

was used to assess the infiltration rate. To do this, the infiltration experiment was performed isothermally at either 1100 or 1200°C, abruptly stopped at different instants, and the samples quickly cooled to evaluate the depth of the infiltrated layer. After dismounting the experimental apparatus, samples were extracted from the alumina powder bath and examined. In order to establish the reaction layers thickness formed during the heating step (up to the infiltration temperature), reference samples were obtained by heating, up to 1100 or 1200°C respectively, and quickly cooled. As during each experiment, performed according the scheme in Fig. 1, infiltration occurs through the glass bar in the longitudinal direction only, the border between the reacted and the not-reacted parts of the specimen can be appreciated to the naked eye and the length of the bar traveled by the infiltrating alloy can be easily measured by a calliper. Finally, the thickness value of the infiltrated layer was measured.

Composite specimens for mechanical tests were obtained by submersion of silica glass samples in molten aluminum kept inside an alumina crucible. The thermal cycle adopted for these specimens is shown in Fig. 2.

Both silica glass pre-forms and crucibles containing aluminum were pre-heated to 850°C, in air, using an electric oven, then the silica specimen was immersed into the molten metal, the temperature was raised to 1100°C and then held until infiltration was complete.

A slow cooling step from 1050 to 950°C was adopted in order to avoid any damage to alumina crucible. After a slow cooling, to 700°C, the composite sample was taken out of the metal bath and further cooled inside the oven until about 200°C, and then it was extracted from the furnace.

The formation of the composite material occurs according to the displacement reaction:

$$3SiO_2 + 4Al \rightarrow 2Al_2O_3 + 3Si \qquad (1)$$

The reaction (1) was also investigated by Differential Thermal Analysis (using a Perkin Elmer-DTA7). To this purpose, powders of silica glass and aluminum (or an aluminum-silicon alloy) were mixed, pressed and heated to 900°C, in Ar, at different heating rates (5, 10, 20 and 40°C/min, respectively). The results were processed according to the Ozawa's method [17, 18], in order to calculate the activation energy (E) for the

displacement reaction according to the equation:

$$\log \phi = -0.4567 \cdot \frac{E}{R \cdot T} + C \qquad (2)$$

where, T is the temperature in Kelvin, which allowed a prefixed fraction of material (for example 0.5) to be transformed during the tests performed at various values of scanning rate ϕ (K/min), R is the universal gas constant, and C a constant, whose value depends on the pre-fixed fraction of transformed material.

The temperature at which the reaction occurs increases along with the heating rate, as always happens for thermally activated transformations.

DTA scans, performed with each heating rate (Φ_i), allow for measuring the temperature values (T_i) corresponding to the transformation of a pre-fixed fraction of silica (for example = 0,5). By plotting these values of log Φ_I against $1/T_i$ the Ozawa's graphic is obtained. The activation energy was calculated from the slope of this plot, which is equal to $-0.4567 \cdot E/R$.

2.2. Material characterization

The microstructure of C^4 material was investigated, with the aim of explaining its mechanical features and in order to better understand the reactive penetration mechanism. The microstructure of the composite was analyzed using optical and scanning electron microscopy, the latter coupled with energy dispersive X-ray spectroscopy (EDS) for compositional evaluations. The samples were sectioned and mechanically polished without etching for microstructure investigations. Composite phases were identified by X-ray diffraction (Cu K_α radiation, Philips PW3040 instrument equipped with a monochromator). The sample dimensions were measured before and after the reactive infiltration process. The ceramic percentage in C^4 was determined by weighing the alumina remaining after dissolution of metal by acid etching. To this purpose a thin slice of composite (few mm thick) was etched by an HCl solution for 24 h.

Open porosity of C^4 samples was studied by mercury intrusion porosimetry (Carlo Erba PO 2000 equipment, operating at a pressure up to 2000 bars, suitable for detecting pore sizes ranging between 0.0037 μm and 58 μm). The final composite density was determined from the ratio between the specimen weight (measured in air) and the buoyancy measured by immersing the specimen in water. The comparison between the measured density and the theoretical one allowed for calculating the total material porosity.

Surfaces of fracture mechanics samples were analyzed by using the scanning electron microscope in order to investigate, in terms of mechanism of rupture, effects of different phases constituting composite materials.

2.3. Mechanical properties

An indirect evaluation of the strength of interfacial bond between metal and ceramic networks was made on the basis of dilatometric measurements. The thermal expansion coefficient of round C^4 bars (7.65 mm diameter, 40 mm length) was measured in the temperature range of 30–230°C (Netzsch, Dil402) and compared with those of pure aluminum and alumina. Generally speaking, for metal-ceramic composites a progressive decrease of thermal expansion is expected with the increase of ceramic content, provided that a strong interfacial metal-ceramic bond exists. However, the thermal expansion of such composites also depends on the shape of ceramic reinforcement.

Specimens $5 \times 10 \times 50$ mm^3 were submitted to three points bending test, performed at a constant rate-crosshead speed of 0.1 mm/min- using a Sintech 10D equipment, in order to obtain MOR data. This equipment was also used for compression, and tensile tests. For compression tests, cylinders 7.65 mm diameter and 12 mm long were used, while for tensile tests round bars 7.65 mm diameter and 70 mm long were used. An extensometer was used to measure the axial strain during tensile tests. Elastic modulus was evaluated by an impulse excitation technique involving the analysis of the transient composite natural vibration (GrindoSonic MK5 instrument).

Unnotched specimens $5 \times 10 \times 50$ mm^3 were submitted to instrumented Charpy testing (ATS-FAAR Izod-Charpy apparatus with a 34.3 N hammer).

Vickers hardness measurements (load 196.2 N) were performed on the cross section of composite samples.

The fracture toughness (K_{Ic}) was evaluated at room temperature using three point bending samples (specimen sizes: $4.5 \times 9 \times 50$ mm^3). Blunt SENB specimens (notch: 3 mm height, and 0.15 mm notch tip radius) were used. Span length and crosshead speed were 36 mm and 0.5 mm/min, respectively. The geometry of the fracture samples was the same as used in previous studies [19, 20] to measure the fracture toughness of metal matrix composite materials produced using different fabrication technologies (casting and powder metallurgy). Actually, in the case of these last MMC composites, characterized by a different kind (SiC particles) and percentage of reinforcement (about 30% vol.) with respect to C^4 composite materials, both precracked and blunt notched specimens (notch tip radius = 0.15 mm) were successfully used (according to 399 ASTM standard). Therefore, notwithstanding the composite produced by liquid displacement is mainly constituted with ceramic phase, the fracture mechanics tests were carried out using this method, originally drawn up for metallic materials. This choice is due to the hope of collecting valid linear elastic K_{Ic} data avoiding using tests specifically prepared for very brittle materials, such as ceramics [21–25]. On the other hand, among these last tests, those based on indentation inducing microcracks (or microflaws), not only are strongly affected by porosity and residual stresses [26], but for C^4 composite are not suitable for determining the toughness, because of the irregular growth of cracks in different directions; cracks easily run within the ceramic network but are stopped or deflected at the interfaces with metal matrix.

3. Results and discussion

3.1. Reactive metal penetration process

Reactive penetration of molten aluminum in the silica glass preform resulted in the formation of a co-continuous Al_2O_3-Al(Si) composite containing 63% vol. of ceramic. Specimen dimensional changes occurring during the infiltration process were always found to be lower than 0.5%; this shrinkage allows for defining RMP process as a near net shape production method. A total porosity equal to 1.7% was calculated as comparing measured density (3.53 g/cm^3) with the theoretical one of 3.59 g/cm^3, calculated by knowing the composite content of alumina (63% vol.). Furthermore, mercury intrusion measurements showed the presence of open porosity lower than 0.1% vol., with pores smaller than 0.01 μm.

DTA experiments showed that the reaction starts already at low temperature and just above the metal melting point. However infiltration rate measurements showed a too slow kinetic of reaction for practical applications below 800°C. Otherwise, at all the temperatures ranging between 800°C and 1200°C, the molten aluminum spontaneously infiltrates into the glass sample, forming two interpenetrated continuous networks of metal and alumina.

In Fig. 3 results from infiltration tests, performed with the method shown in Fig. 1, are collected. The molten aluminum penetration thickness (after one hour of infiltration) depends on temperature in a complex manner. The infiltration thickness increases with temperature, and achieves values suitable for practical applications, greater than 3.5 mm after 1 h, only in the case of test starting from 1100°C. However, a noticeable maximum in infiltration thickness versus temperature, of about 3 mm after 1 h, was observed at about 800°C. This irregular trend has been previously reported in literature and explained with the formation of γ-alumina at around 800°C, instead of α-alumina, which is the phase generally detected in the C^4 above 1100°C [27]. Surprisingly, XRD analysis of the C^4 composite obtained at 800°C showed that only α-alumina is present at the end of the infiltration process. Probably γ-alumina is, therefore, an intermediate phase only, whose formation enhances the reactive metal penetration speed in an initial process step. The infiltration speed also depends on the composition of the molten aluminum based alloy used. Fig. 3b and c show that the presence of silicon as alloying element in the aluminum alloy slows down the infiltration process; this behavior can be easily explained taking into account that silicon is one of the products arising from the displacement reaction, which promotes infiltration. According to these results, different activation energy values of the displacement reactions were found for different infiltrating alloys: 185 kJ/mol for pure Al and 193 kJ/mol for Al-10%Si alloy respectively (Fig. 4). These results evidence the role played by both temperature (1100°C and 1200°C) and infiltrating alloy composition (Al 99.9 and Al10%Si) on RMP rate. Moreover also other experimental parameters affect the infiltration speed. The comparison of infiltrated thickness in Fig. 3a (measured after tests carried out with the apparatus in Fig. 1) and in Fig. 3b and c (referring to infiltration performed by silica sample submersion in molten metal) shows, in fact, that the thickness achieved after one hour slightly depends on the geometry of apparatus used for sample preparation.

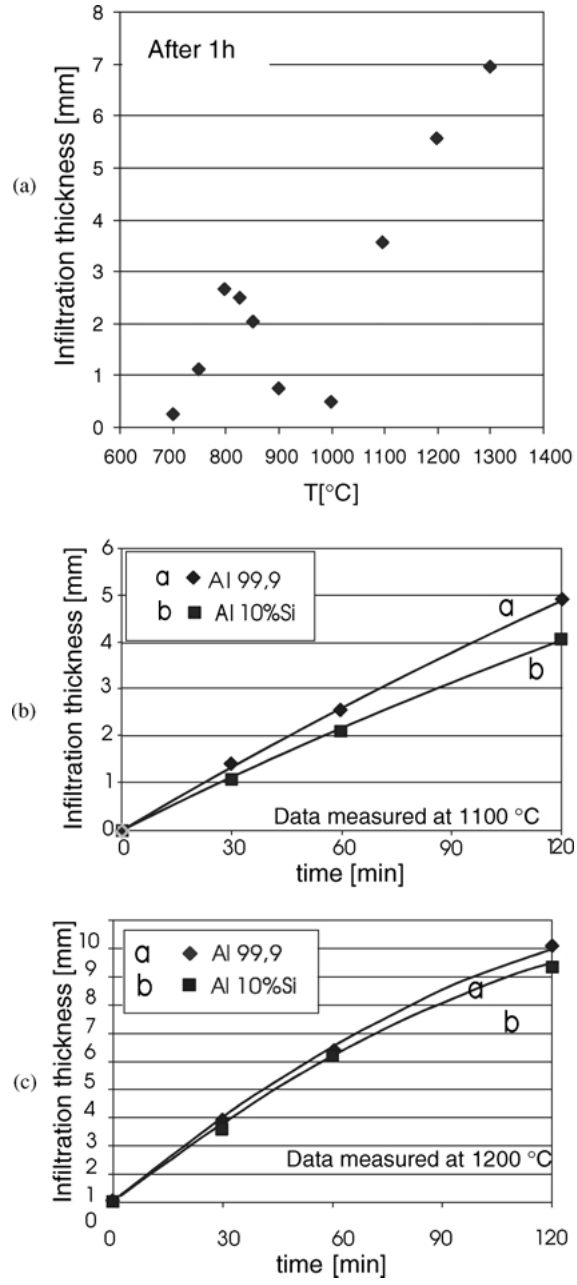

Figure 3 Thickness of infiltrated layer: (a) after one hour of reaction with molten aluminum at different temperatures. Infiltrated layer vs. time for C^4 obtained by using pure Al and Al-10%Si: RMP at 1100°C (b), and RMP at 1200°C (c).

3.2. Composite microstructure

Optical microscopy showed that a co-continuous structure forms at all the infiltration temperatures ranging between 800 and 1200°C, and that the size of alumina particles (linked together to make a ceramic network) increases with the temperature (Fig. 5).

The ceramic network is strictly interpenetrated with continuous interconnected Al zones (Fig. 6b). The aluminum phase is also present in the form of rather stretch

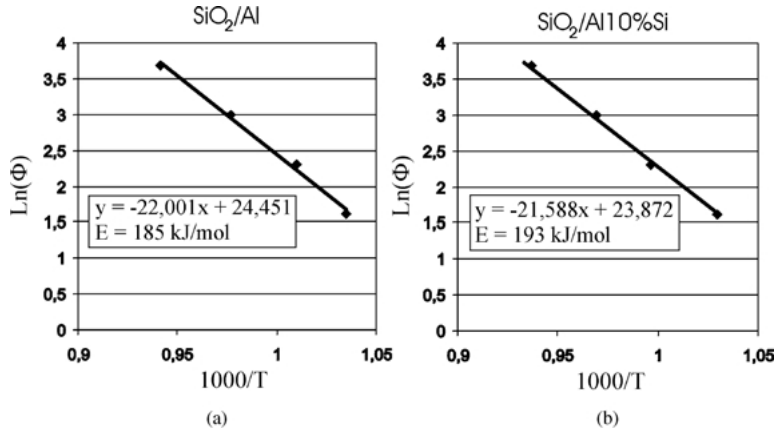

Figure 4 Ozawa's plots for reactive infiltration with pure Al (a) and Al-10%Si (b) computed from DTA results.

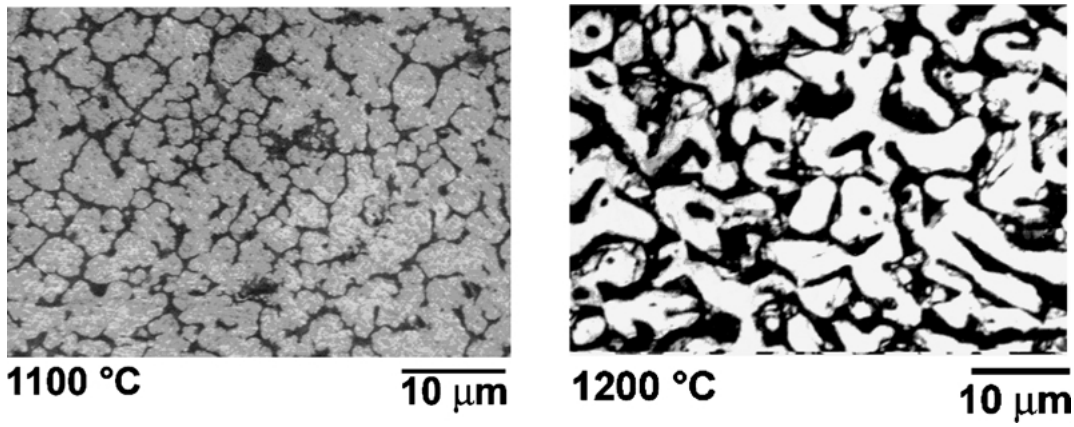

Figure 5 Co-continuous Al/Al_2O_3 networks resulting from RMP at 1100°C and 1200°C.

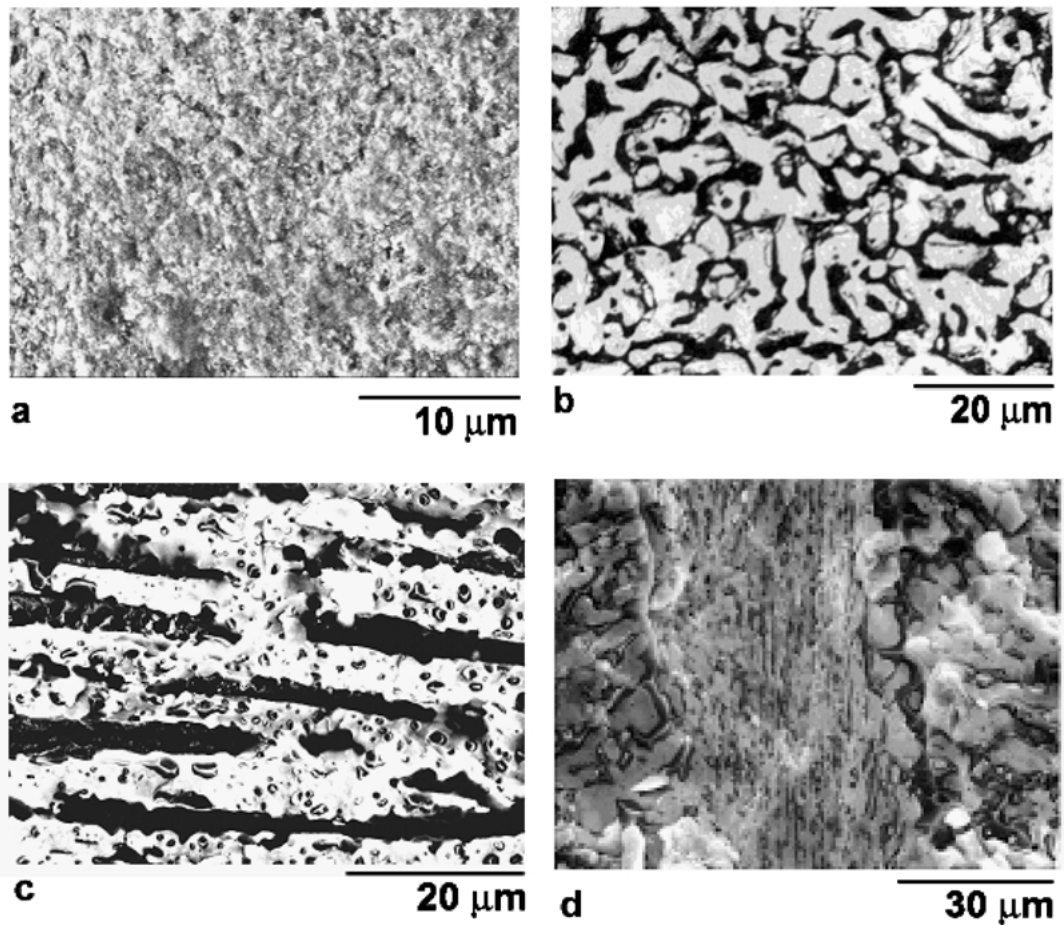

Figure 6 C^4 microstructure: (a) fine structure close to the sample surface; (b) coarse structure generally observed in the major part of the sample; acicular morphology of microstructure grown perpendicular to sample surface (c), and parallel to sample surface grown in the sample center (d).

oriented areas, to form channels, whose direction is consistent with the growth direction of Al_2O_3/Al composite. A strong variation in both the microstructure refinement and the orientation of the metallic phase channels was detected in different parts of the composite cross section. The surface of C^4 specimens is characterized by the presence of alumina crystals much smaller than those observed inside sample (Fig. 6a and b). Both under the sample skin and in the middle of the cross section, an acicular structure can be frequently observed (Fig. 6c and d). This last microstructure is characterized by elongated alumina crystals, respectively growing perpendicular or parallel to the sample surface in zones formed just below the sample skin (Fig. 6c) or at the sample center (where the reaction fronts moving from opposite directions meet Fig. 6d). These morphological changes observed in a composite section can be tentatively explained by taking into account the peculiar advancement mechanism of the reaction front and the silica glass crystallization at the sample core, occurring before infiltration finish. As soon as infiltration began, the reaction between molten metal and silica glass produces the formation of an alumina layer. A volumetric contraction, approximately 25% (resulting from transformation of silica into alumina), causes cracking of glass. These cracks are responsible for a further penetration of aluminum into the SiO_2 precursor (Fig. 7a). According to this infiltration mechanism a convoluted reaction front at the interface between C^4 and silica glass was experimentally observed during the first reaction period (Fig. 8). Above 1100°C, the core of the glassy preform undergoes crystallization before reacting (Fig. 9a and b). Then the external alumina layer results from reaction between glassy silica and molten metal, while the alumina contained in the sample core originates from reaction between crystobalite and molten metal. The alumina crystals arising from the reaction of crystobalite grains are not oriented and coarser than those obtained by reaction of silica glass.

The shrinkage arising from the reaction is the cause for the formation of channels perpendicular to the sample surface in which is localized the metallic phase (Fig. 6c). For this reason below the surface layer, made of small and not oriented crystals, a columnar structure forms. When the reaction fronts, moving from opposite directions, approach the sample center, heavy tensile stresses (resulting from the shrinkage involved in C^4 formation, Fig. 7b and c) may cause the crack of the inner layer of not yet infiltrated silica. These cracks, which grow perpendicularly to the infiltration direction, probably drive the final infiltration step to occur parallel to the sample surface.

The orientation of the microstructure, typical of zones away from the surface of the samples, probably causes a certain anisotropy of the mechanical properties, and therefore the effect of the microstructure morphology in the different zones of the C^4 composite specimens on the crack propagation should be considered evaluating the composite toughness data.

The presence in the aluminum channels of some particles of Si has been also detected. Such particles precipitate from the supersaturated molten Al during the

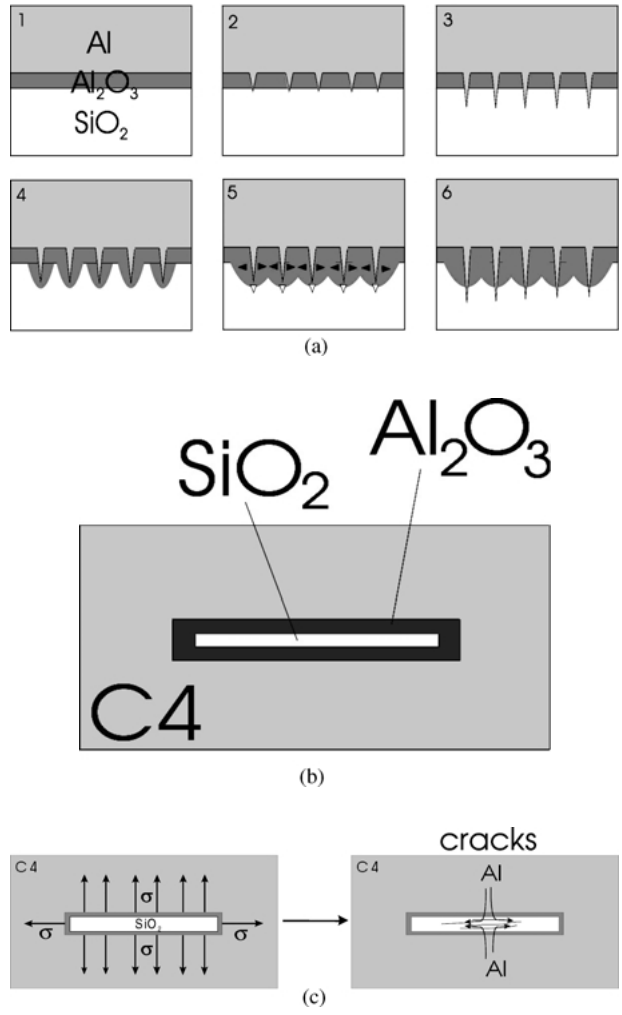

Figure 7 (a) Steps involved in RMP process: (1) a first thin external layer of alumina forms; (2) this layer cracks owing to volume contraction; (3) cracks go on growing towards the silica layer; (4) alumina (in gray) forms at molten cracked/cracked silica interface; (5,6) further shrinkage causes cracks advance in glass. (b) Final step of reactive penetration in thin silica plates: induced thermal stresses cause silica cracking at C^4/silica interface (c).

solidification process. The size of Si particles ranges from 0.5 to 1 micron. Therefore the composite microstructure consists mainly of Al_2O_3 and Al, and, additionally, of small amount of Si in the Al channels. EDS spectra recorded from the ceramic and metallic phases are shown in Fig. 10, in which ceramic phase being essential pure Al_2O_3 and metallic phase containing only small amount of Si. X-ray diffraction patterns of C^4 specimens obtained by reactive penetration of Al or Al-10%Si in silica glass samples confirm the presence only of these three phases in the composite (Fig. 9c and d).

The average silicon content in the metal part of the composite appreciably changes during the advancement of the reactive penetration process. This feature was appreciated by carrying out electron microprobe analyses on the co-continuous layer grown in the external part of a silica sample after partial infiltration (reaction stopped by pulling out sample from metal bath and rapid cooling to room temperature). Analyzing such a specimen at different distances from the reaction front it was obtained the concentration profiles for aluminum, silicon and oxygen reported in Fig. 11. Moving from

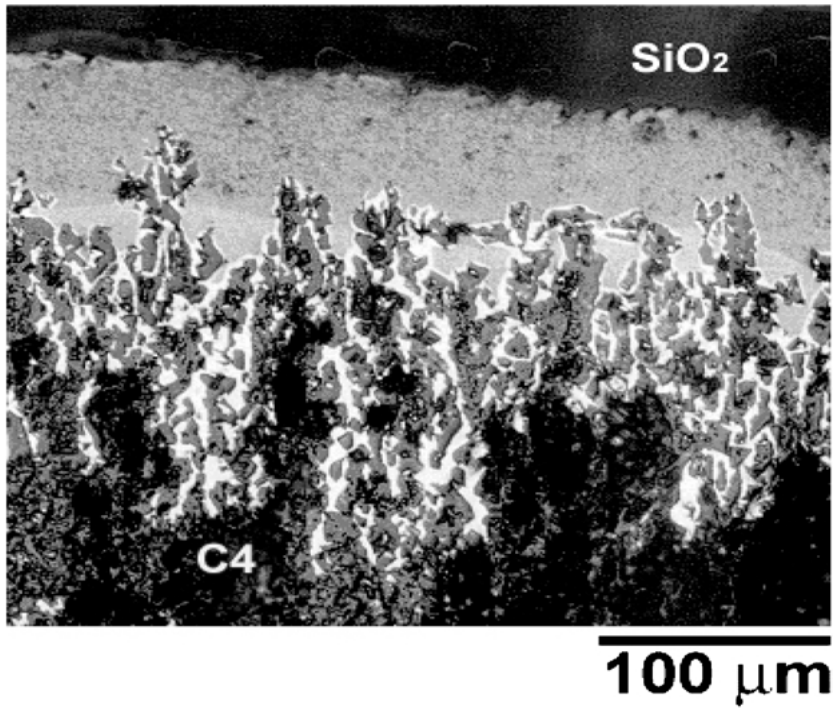

Figure 8 Convoluted reaction front observed when the RMP process stopped before the complete sample infiltration.

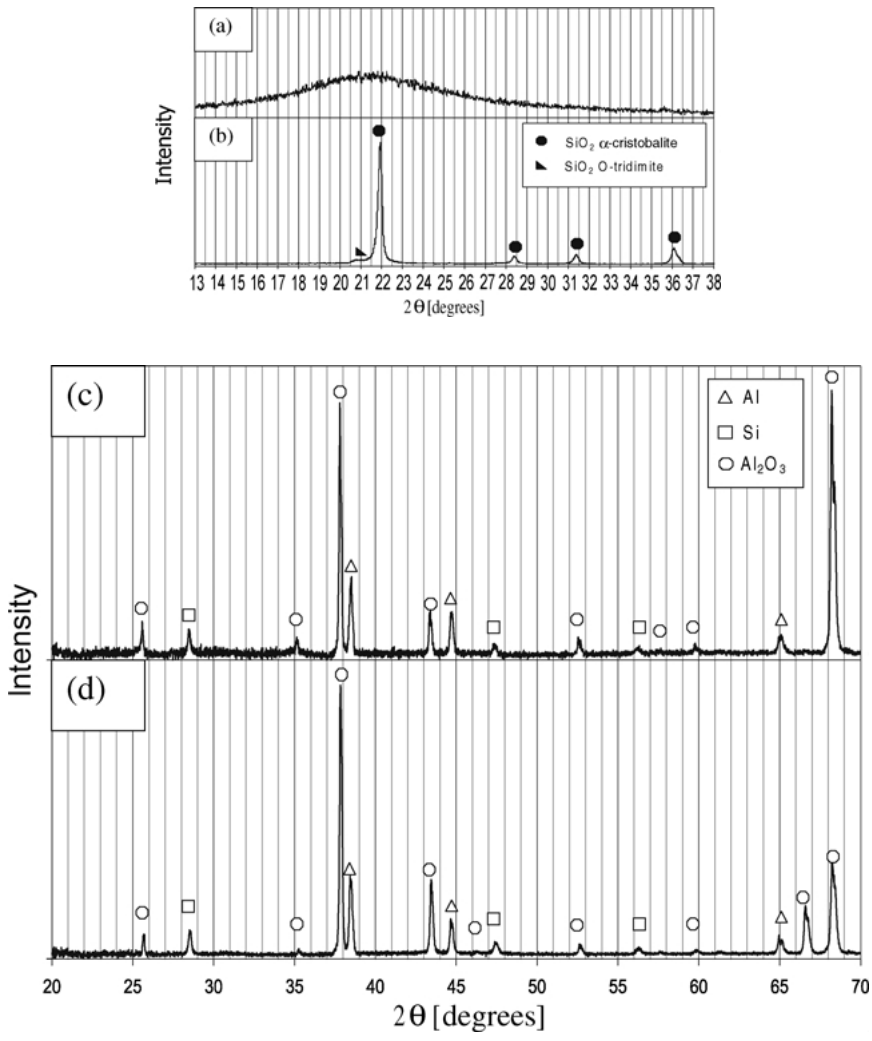

Figure 9 XRD patterns of silica: (a) at the beginning of RMP process; (b) after 1 h at 1200°C. XRD patterns of C^4 composite obtained by RMP carried out by using: (c) pure Al; (d) Al-10%Si alloy.

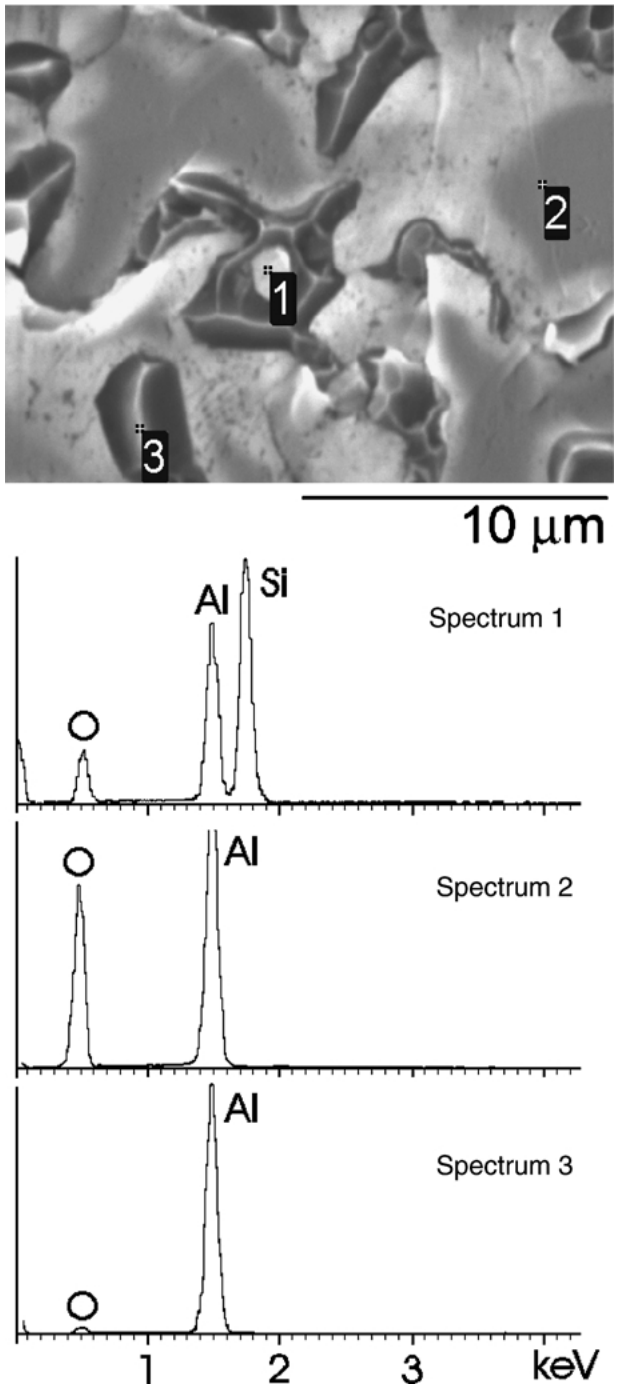

Figure 10 EDS analyses of: Si base precipitates (spectrum 1); alumina (spectrum 2); cracked alloy (spectrum 3).

the reaction front towards the sample surface, the silicon content progressively decreases while aluminum concentration changes in the opposite manner. The oxygen concentration was found almost constant, which is consistent with its presence in alumina only. Conclusively, the liquid channels serve as paths not only for the continuous supply of molten aluminum but also for the diffusion of the produced Si away from the silica. Thus, the formation of liquid channels is essential for further proceeding of the displacement reaction and for the growth of the composite microstructure. Owing to the progressive diffusion of silicon towards the metal bath, its concentration inside the metal component of C^4 becomes practically constant at the end of the infiltration process. This final silicon concentration only

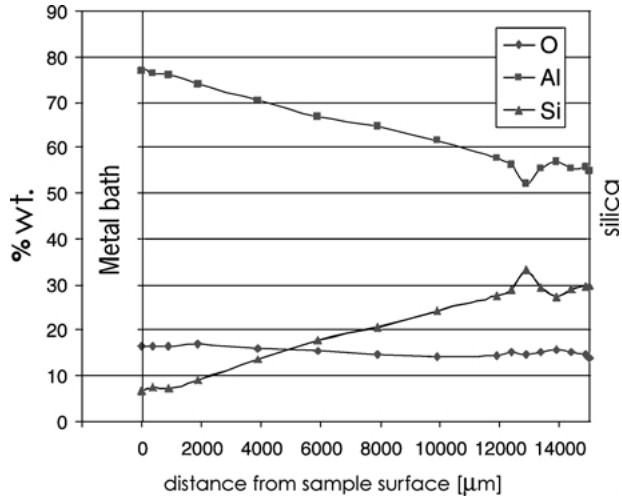

Figure 11 Concentration curves of Al, Si and O in a C^4 layer grown in a partially infiltrated SiO_2 specimen.

depends on the ratio between the volume of C^4 specimen and that of the molten metal bath used. The experimental conditions adopted in this work resulted in final silicon concentrations (inside the metal component of the material) of about 5% or of about 15%, respectively when pure aluminum or Al-10%Si alloy were used as infiltrating metal bath.

No tendency for any reactions or instabilities at the interface between the metallic and ceramic phases has been detected.

3.3. C^4 Mechanical behavior

3.3.1. Thermal expansion

Thermal expansion measurements were proved to be suitable for investigating the strength of interfacial bonds in metal ceramic composites. In fact, only if these bonds are sufficiently strong, the composite shows thermal expansion coefficient values (CTE) between those of pure ceramic and metal ones (which are one order of magnitude different). The weakening of interfacial bonds, for instance arising from thermal stresses occurring during thermal cycling, causes an increase of composite CTE, which progressively approaches that of unreinforced metal with the advancement of interface damage [27]. This method for investigating interfacial bond strength seems particularly useful in the case of co-continuous composites. Actually, for these materials it seems difficult to use most of the conventional methods generally adopted for evaluating the interfacial strength in composites (like pull out or push out methods), because the ceramic particles are interconnected in all directions, then they may glide with respect to the metal only after the breakage of these connections. The thermal expansion curve of Al-Al_2O_3 C^4 composite is compared with those of pure aluminum and pure alumina in Fig. 12. Linear expansion coefficient of composite (10.7 ppm/°C, measured between 30 and 230°C) is even lower than that computed for C^4 composite by the rule of mixture on the basis of Al and Al_2O_3 CTEs (22 and 6.5 ppm/°C, respectively, in the same temperature range). This result shows that

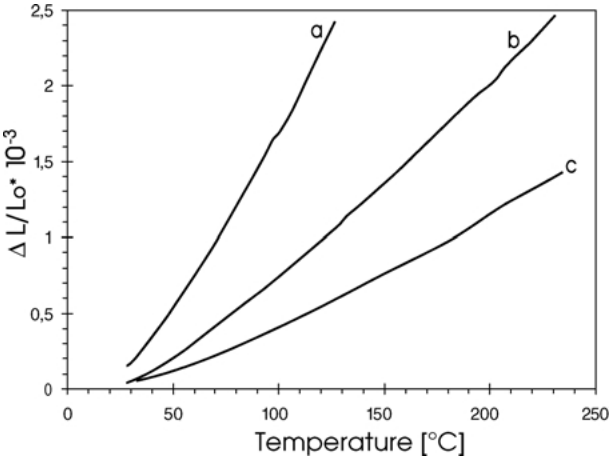

Figure 12 Linear thermal expansion curves for: (a) pure Al, (b) C^4 Al/Al_2O_3 composite, and (c) pure Al_2O_3.

strong interfacial ceramic-metal bonds exist and that final composite microstructure, characterized by a continuous ceramic network, concurs to lower down the composite thermal expansion.

3.3.2. Bending, compression and tensile properties

Some mechanical features of the co-continuous 63%Al_2O_3/37%Al composite are listed in Table 1. Owing to its high ceramic content, C^4 material shows a linear elastic behavior with strain at rupture lower than 0.1% only and a very high stiffness.

The material displays a good compressive strength and an appreciable module of rupture, while its tensile strength is rather poor. The average hardness value is consistent with the high alumina concentration. Moreover this property is also affected by the microstructure, which is not completely homogeneous in all the composite parts, as discussed in a previous section.

The general mechanical behavior of C^4 composite seems mainly controlled by the high ceramic concentration and, at least with reference to tensile strength, by the presence of residual porosity too.

3.3.3. Fracture toughness and impact resistance

The fracture energy measured for C^4 composites by Charpy impact test (1.3 J/cm^2) is consistent with that reported in a previous paper [27] for a conventional Al6061-SiC composite. The presence in Al6061/SiC composite of 20%vol. of ceramic lowers the impact

TABLE I Mechanical properties of the investigated composite (all data are averaged of at least five tests).

Compression		Bending	Tensile			
Strength (MPa)	Strain (%)	MOR (MPa)	UTS (MPa)	Strain (%)	Young Modulus[a] (GPa)	Vickers hardness
773	<0.1	280	122	<0.1	202	448

[a]Measured from natural vibration frequency of composite.

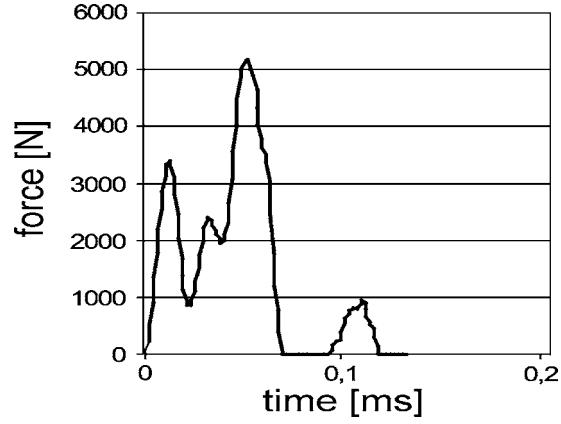

Figure 13 Force vs. time of C^4 composite submitted to Charpy impact test.

energy of this last composite with respect to unreinforced aluminum (30 J/cm^2) down to about 5 J/cm^2 only. The presence of 63% vol. of ceramic in C^4 composite, which is more than three times the ceramic content in Al6061/SiC, of course decreases the impact energy well below 5 J/cm^2. Nevertheless, the Charpy force-time curves showed that the continuous microstructure of C^4 material probably provides some toughening mechanism (Fig. 13). Actually, this experimental curve is structured (like those of some fiber-reinforced composites), showing that after a first material damage (very likely due to cracking of ceramic network), a further work and a related force increase are necessary for sample fracture.

Fracture mechanics tests have been also carried out in order to obtain toughness data representative of the investigated material and independent from the specimen geometry.

SENB tests allowed for measuring a C^4 critical value of the stress intensity factor of 5.3 ± 0.6 MPa$\sqrt{\text{m}}$. This result is consistent with toughness values reported in the literature for interpenetrating phase composites having aluminum as metal phase and alumina as reinforcement [10] and obtained using the ASTM 399 standard as reference. The fracture toughness of the composite was found twice than that corresponding to the ceramic phase, which is about 2.6 MPa$\sqrt{\text{m}}$ [25]. Toughening effect of the continuous aluminum network in the microstructure is therefore demonstrated.

3.3.4. Fractography

The fracture surface of the tested fracture mechanics composite samples displayed the interconnected aluminum effect (Fig. 14).

Changing in fracture surface morphology, from cleavage (typical mechanism of fracture for ceramic materials) to cleavage plus dimples (the last typical of ductile fracture mechanism and manifest inside the metallic ligaments), indicates the toughening effect of three-dimensional interpenetrating aluminum in ceramic (Fig. 15). The severe deformation of the metallic phase before failure suggests that alumina fails first, and the aluminum phase attempts to hold the remaining material together before failing in a ductile manner. Therefore, it is clear that the ceramic phase provides

Figure 14 Example of fracture surface showing Al_2O_3 and Al phases interpenetrated.

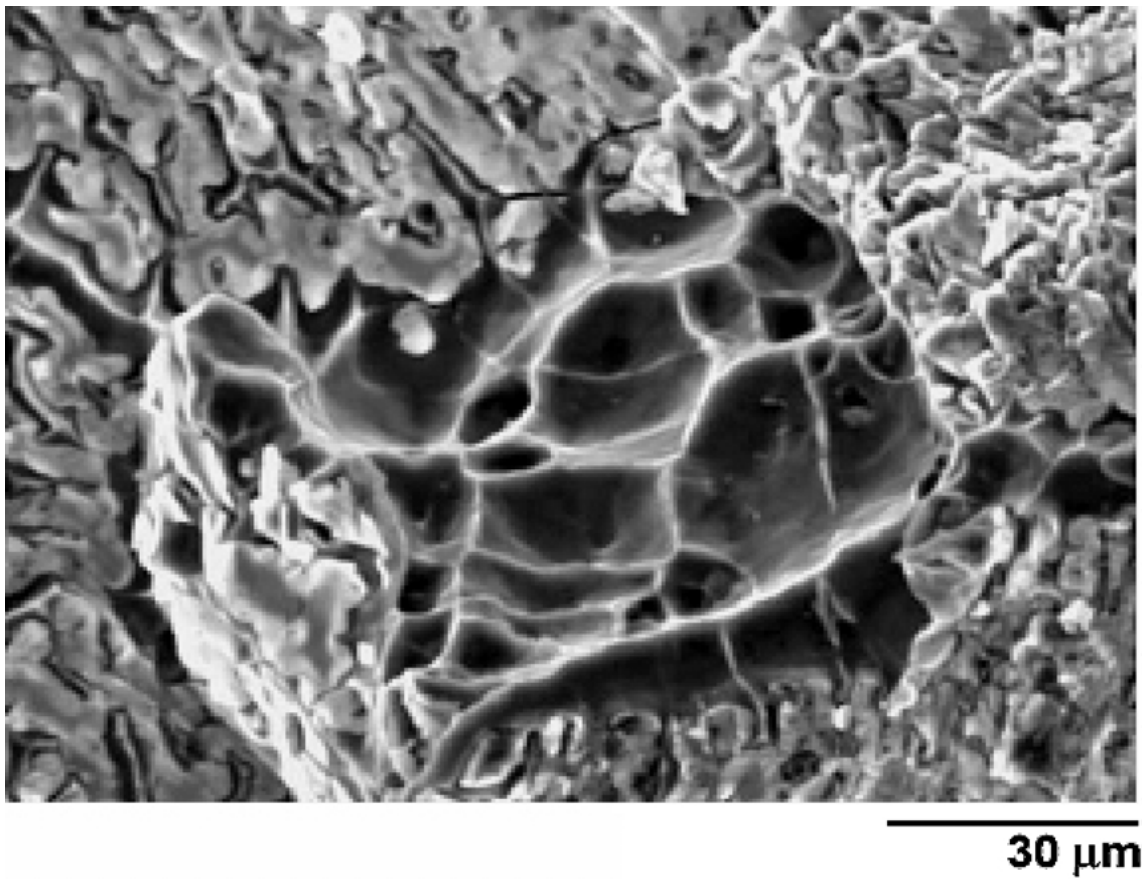

Figure 15 Ductile fracture (microdimples) characterizing a zone in which the metallic phase is prevalent.

much of the initial mechanical resistance and stiffness, while the metallic phase allows plastic deformation and supports the material after the ceramic phase has failed.

On the other hand, SEM examination of fracture surfaces of tensile and bending specimens shows that the metal component undergoes significant plastic deformation before failure, which might result in a toughening effect.

4. Conclusions

Composite samples α-Al_2O_3/Al (Si) with an high ceramic content and a co-continuous structure (due to the interpenetration of two different networks) can be obtained in the temperature range from 800 to 1200°C by reactive metal penetration of silica glass. The speed of pure aluminum penetration in silica glass becomes sufficiently high for industrial application at temperature over 1000°C.

As silicon forms during the displacement reaction, which involves silicon dissolution in the infiltrating molten metal, pure aluminum allows for higher reaction speed than Al-Si alloys. Calculated activation energy of the displacement reaction concurs to assess that the total RMP process is mainly controlled by the reaction between molten metal and silica.

In spite of its co-continuous character, the composite microstructure is not completely homogeneous: columnar aluminum channels form just below the sample skin as well as at the sample center.

This feature, the progressive increase of grain size observed with increasing distances from the sample surface and a residual porosity exceeding 1% vol., affect the mechanical behavior of this composite (also causing the scattering of experimental results).

Strong bonds at the metal/ceramic interface and the continuous ceramic network, which hinders metal plastic flow, allows for very low thermal expansion, high stiffness, low strain at failure and appreciable bending and compression strength.

Both impact and toughness tests showed that the metal component (less than 40%) provides an appreciable toughness increase with respect to traditional ceramics.

Increase in the fracture mechanics data recorded testing the co-continuous Al-Alumina composite (5.3 $MPa\sqrt{m}$), with respect to the typical toughness data characterizing merely the ceramic phase (2.6 $MPa\sqrt{m}$), is the result of two different phenomena: a crack blunting, due to the plastic deformation of metallic zones, and the subsequent crack propagation. This last one is governed by ligament breakage of the metallic phase, along with reinforcement fracturing due to cleavage.

References

1. G. MARSH, *Mater. Today* **3** (2000) 21.
2. C. BADINI, M. LAVECCHIA, P. FINO and P. COBELLI, *Mater. Sci. Tech.* **16** (2000) 681.
3. A. J. SHAKESHEFF and C. PURDUE, *ibid.* **14** (1998) 851.
4. J. RINGNALDA, M. C. BRESLING, J. SEEGER, D. LE JEUNE, G. S. DAHEN and H. L. FRASEN, SAE Technical Paper Series 940850 (1994) p. 83.
5. P. KUMAR, N. A. TRAVITZKY, P. BEYER, K. H. SANHAGE, R. JANSSEN and N. CLAUSSEN, *Scripta Mater.* **44** (2001) 751.
6. F. WAGNER, D. E. GARCIA, A. KRUPP and N. CLAUSSEN, *J. Europ. Ceram. Soc.* **19** (1999) 2449.
7. B. V. CHAMBERS, M. L. SELEZNEV, J. A. CORNIE, S. ZHANG and M. A. RYALS, SAE Technical Paper Series 960162 (1996) p. 107.
8. T. ZEUNER, P. STOJANOV and P. SAHM, *Mater. World* **1** (1998) 17.
9. G. S. DAEHN, B. STARCK, L. XU, K. F. ELFISHANY, J. RINGNALDA and H. L. FRASER, *Acta Mater.* **44** (1996) 249.
10. G. W. HAN, D. FENG, M. YIN and M. J. YE, *Mater. Sci. Engin.* A **225** (1997) 204.
11. W. LIU and U. KOESTER, *ibid.* A **210** (1996) 1.
12. M. C. BRESLIN, J. RINGNALDA, L. XU, M. FULLER, J. SEEGER, G. S. DAEHN, T. OTANI and H. L. FRASER, *ibid.* A **195** (1995) 113.
13. W.-P. TAI, T. WATARI and T. TORIKA, *Amer. Ceram. Soc. Bulletin* **76** (1997) 86.
14. L. CESCHINI, G. S. DAHEN, G. L. GARAGNANI and C. MARTINI, *Wear* **216** (1998) 229.
15. V. IMBENI, I. M. HUTCHINGS and M. C. BRESLIN, *ibid.* **233–235** (1999) 462.
16. L. CESSCHINI, A. MORRI, G. SAMBOGNA, M. C. BRESLIN and M. FULLER, *Int. J. Mat. Product. Techn.* **17** (2002) 165.
17. T. OZAWA, *J. Therm. Anal.* **2** (1970) 301.
18. *Idem.*, *ibid.* **7** (1975) 601.
19. G. M. LA VECCHIA, C. BADINI and P. COBELLI, in "Computer Aided Assessment and Control," edited by A. P. S. Salvadurai and C. A. Brebbia (WIT Press Southampton, Boston, 2000) p. 425.
20. G. M. LA VECCHIA and F. D'ERRICO, *Int. J. Mater. Product. Techn.* **17** (2002) 261.
21. G. D. QUINN, R. J. GETTINGS and J. KÜBLER, *Ceram. Eng. Sci.* **15** (1994) 846.
22. B. ROEBUCK, E. BENNET, L. LAY and R. MORRELL, in Measurement Good Practise Guide No. 9, National Physical Laboratory (1998).
23. R. F. BENNISION and B. R. LAWN, *J. Mater. Sci.* **24** (1989) 3169.
24. P. CHANTIKUL, G. R. ANSTIS, B. R. LAW and D. B. MARSHALL, *J. Amer. Ceram. Soc.* **64** (1981) 539.
25. H. MEREDITH and P. L. PRATT, *Proc. British Ceram. Soc.* **20** (1972) 107.
26. M. SAKAI and R. C. BRADT, *Int. Mater. Reviews* **38** (1993) 53.
27. C. BADINI, M. LA VECCHIA, A. GIURCANU and J. WENHUI, *J. Mater. Sci.* **32** (1997) 921.

Received 4 December 2002
and accepted 9 June 2003